UCRL-JC-118285
PREPRINT

IR DIAL PERFORMANCE MODELING

E. T. Scharlemann

Lawrence Livermore National Laboratory

This paper was prepared for
the Proceedings of the 1994 CALIOPE ITR Conference
held May 26-28, 1994, in Livermore, California

July 1994

IR DIAL PERFORMANCE MODELING

E. T. Scharlemann
Lawrence Livermore National Laboratory, Livermore, CA 94551

Abstract. We are developing a DIAL performance model for CALIOPE at LLNL. The intent of the model is to provide quick and interactive parameter sensitivity calculations with immediate graphical output. A brief overview of the features of the performance model is given, along with an example of performance calculations for a non-CALIOPE application.

As an essential part of understanding the potential and problems of IR DIAL for CALIOPE, we are developing a numerical simulation model for the performance of a DIAL-based remote sensing system. The simulation is being constructed with simple but plausibly realistic models for all the important phenomena that we expect to affect DIAL performance, and in such a way that each piece can be easily upgraded as field data becomes available. The intent is to provide quick and interactive parameter sensitivity calculations with immediate graphical output.

Atmospheric propagation in the simulation is based on the techniques and models developed by Phillips Laboratories for FASCOD3P (atmospheric models, Voigt-profile approximations), LOWTRAN7 (aerosol models), and BACKSCAT (aerosol backscatter phase functions). The HITRAN database is used for absorption line parameters; a subset of the database, as required for a specific simulation, is extracted and reformatted by intermediate programs. Laser absorption is calculated using Voigt line profiles for each included atmospheric species, integrated through model atmospheres borrowed from LOWTRAN7. The model atmospheres include profiles for pressure, temperature, water vapor content, and aerosol type, content, and scattering vs. altitude. The pressure and temperature sensitivities of the line strengths and widths (hence cross-sections) are included. The main atmospheric absorption phenomenon not yet treated is the continuum absorption (by water vapor, CO_2, N_2, etc.). Various integrals of the atmospheric structure parameter C_n^2 are evaluated; they serve primarily as an indication of the potential importance of turbulence on beam spread and transverse beam irradiance modulation ("beam breakup").

The simulation treats DIAL measurements based on diffuse target, aerosol, or retroreflector backscattering and on localized Gaussian plume or distributed absorption (*e.g.*, atmospheric water vapor, see the simulation example below). Diffuse target backscattering is characterized by a reflectivity and a return speckle pattern determined by the target spot size; *i.e.*, return speckle cell size taken to be $\lambda R/D$, where λ is the signal wavelength, R the range, and D the target spot diameter. The speckle cell size enters into the determination of the final signal-to-noise ratio through the assumption that speckle introduces an rms pulse-to-pulse signal fluctuation of ~1/√(number of speckle cells in receiver aperture) relative to the signal mean. This assumption is probably valid for laser pulse repetition intervals that exceed either a characteristic atmospheric fluctuation time or the time to sample a new speckle pattern because of platform motion.

Simple parameterized models for the receiving telescope, cold filter, and detector are included, with the detector and its preamplifier defined by quantities that are quoted by detector and amplifier manufacturers; *e.g.*, D*, NEP (noise equivalent power), or spectral density of an amplifier input noise voltage (nV/√Hz) or current (pA/√Hz). Where possible, the detector parameters are taken from manufacturers' specification sheets.

Simulation outputs – all graphical – include calculations of signal-to-noise and carrier-to-noise ratios, measurement uncertainty due to atmospheric temperature uncertainty or noise effects, and probability of detection for specified release rate and probability of false alarm. Presently, the probabilities of false alarm and detection are calculated assuming Gaussian statistics, a good assumption for instrumental and speckle noise (assuming many speckle cells in the receiver aperture) but not a good assumption when the data is the ratio of two noisy quantities. The graphical outputs go simultaneously to an X Window on a UNIX workstation and to a PostScript file for later printing.

Figures 1-4 illustrate some results from the simulation for a non-CALIOPE application, the determination of water vapor concentration from a high-flying UAV with two-line mid-IR DIAL. The UAV is assumed to be looking directly down from 20 km altitude, and carrying a 35-cm receiver telescope and a 5 W average power (100 Hz) laser operating in the water-vapor band around 930 nm. Direct detection by a silicon avalanche photodiode with a transimpedance preamplifier and a two-minute integration time are assumed; the noise parameters used were obtained by Nils Carlson from EG&G for their Si APD. The quantities plotted in the figures as a function of altitude are (a) relative uncertainty of water vapor concentration due to system signal-to-noise, (b) the relative uncertainty due to a 10 K uncertainty in the local temperature (temperature insensitive lines have been chosen to keep this contribution to the uncertainty small[1,2]), and (c) the integrated two-way absorption from the UAV to the altitude being probed. The relative uncertainty in the water vapor concentration depends on many factors, including the atmospheric model — primarily the temperature, water vapor concentration, and aerosol extinction and backscatter, but that, of course, is the reason for doing a simulation.

The Figures show results of the simulation for DIAL measurements at four separate water lines, from very strong to fairly weak. Lines of different strength probe different regions of the atmosphere. The strongest line at 10687.363 cm^{-1} is needed to get good measurement accuracy in the stratosphere, where there just isn't much water vapor. Light at that frequency, however, is all absorbed above 10-km altitude, so weaker lines are needed to probe to lower altitudes, farther from the UAV. The altitude range covered by each line is evident from the plots, with the weakest line at 10678.982 cm^{-1} permitting measurement all the way down to the ground (although in this particular simulation, ground reflection is not included).

This simulation model is being applied to the plume release experiments to be performed at RSTR. As data is acquired from these experiments, and from their predecessors at Site 300, the model will be upgraded to incorporate the many effects that we don't presently understand.

Acknowlegment

This work was performed under the auspices of the U.S. Department of Energy by Lawrence Livermore National Laboratory under Contract W-7405-Eng-48.

References

1. T.D. Wilkerson and G.K. Schwemmer, *"Lidar Techniques for Humidity and Temperature Measurement," Optical Engineering*, **21**, 1022 (1982).

2. E.V. Browell, S. Ismail and B.E. Grossman, *“Temperature Sensitivity of Differential Absorption Lidar Measurements of Water Vapor in the 720-nm Region,” Applied Optics*, **30**, 1517 (1991).

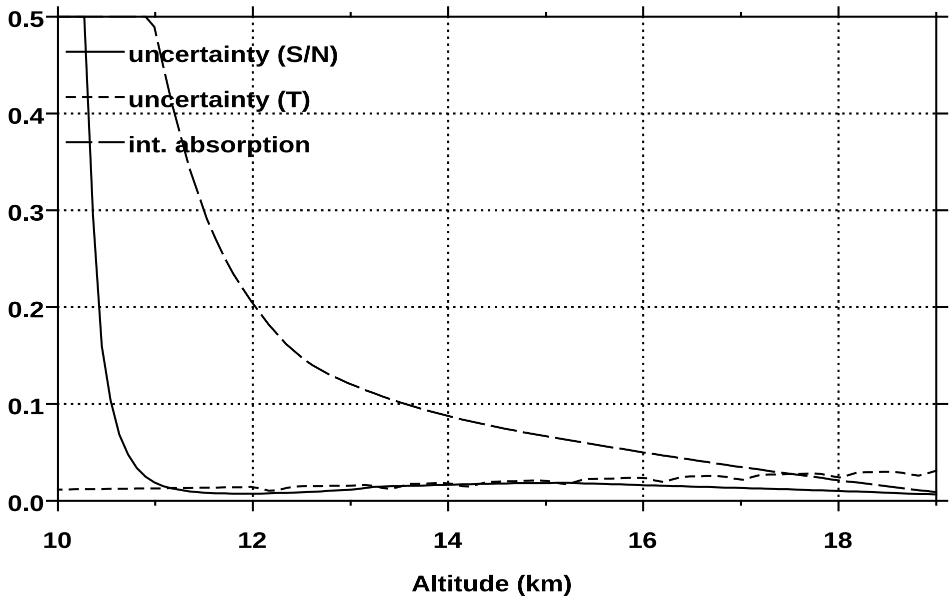

Figure 1. Simulation of a 2-line DIAL measurement of water vapor concentration from 20-km altitude looking downward. The quantities plotted are the relative uncertainty of water-vapor concentration due to system signal-to-noise ratio, the relative uncertainty due to the temperature sensitivity of the chosen absorption line (at 10687.363 cm^{-1}), and the integrated round-trip absorption from the lidar to the altitude being probed.

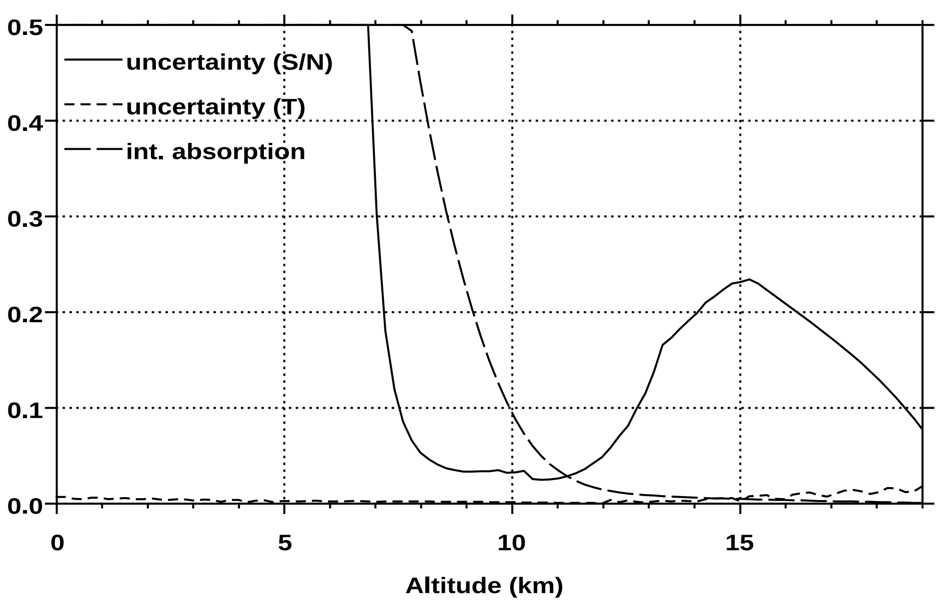

Figure 2. The same as Figure 1 for a weaker line at 10709.86 cm^{-1}.

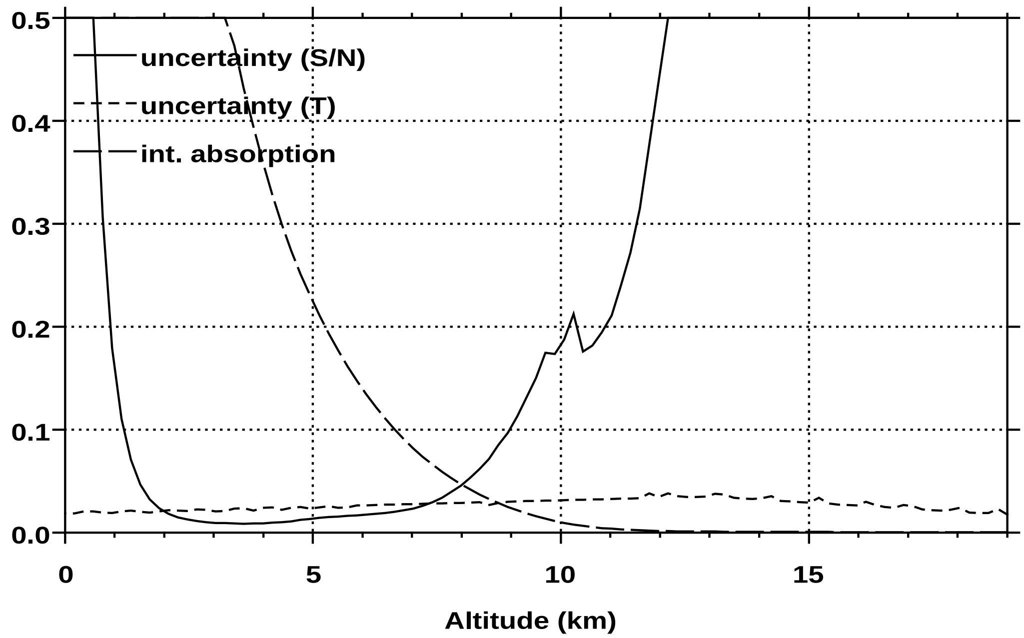

Figure 3. The same as Figure 1 for a yet weaker line at 10733.578 cm^{-1}.

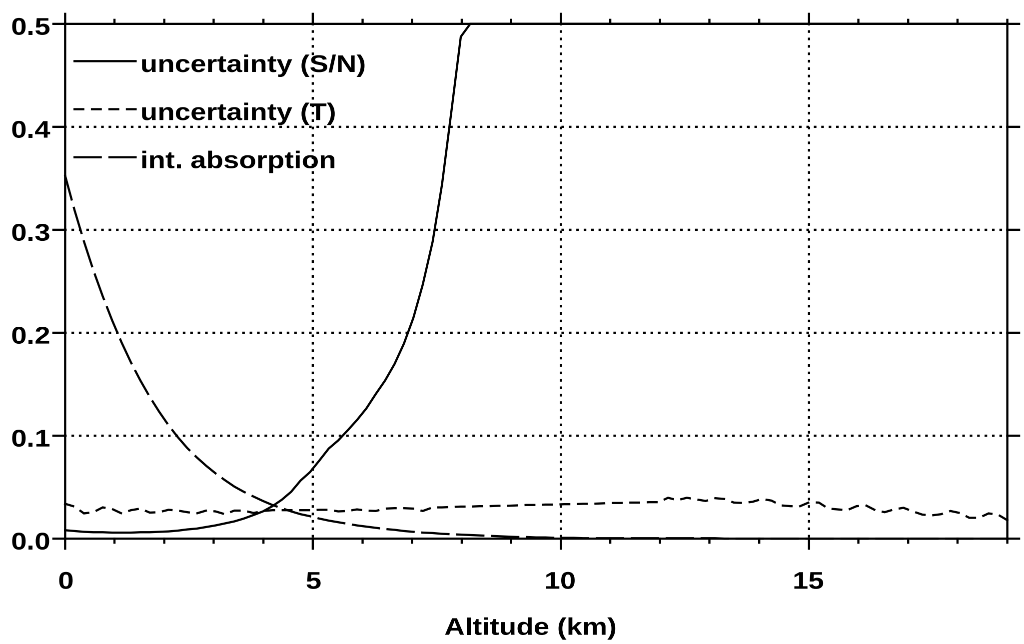

Figure 4. The same as Figure 1 for a very weak line at 10678.982 cm^{-1}, permitting accurate water-vapor concentration down to near sea level (for this particular simulation, reflection from the surface is not included.)

Technical Information Department • Lawrence Livermore National Laboratory
University of California • Livermore, California 94550